

Flipped $SU(5)$: unification, proton decay, fermion masses and gravitational waves

Stephen F. King^{a 1}, George K. Leontaris^{b 2}, Ye-Ling Zhou^{c 3}

^a *School of Physics and Astronomy, University of Southampton,
SO17 1BJ Southampton, United Kingdom*

^b *Physics Department, University of Ioannina, 45110, Ioannina, Greece*

^c *School of Fundamental Physics and Mathematical Sciences,
Hangzhou Institute for Advanced Study, UCAS, Hangzhou 310024, China*

Abstract

We study supersymmetric (SUSY) flipped $SU(5) \times U(1)$ unification, focussing on its predictions for proton decay, fermion masses and gravitational waves. We performed a two-loop renormalisation group analysis and showed that the SUSY flipped $SU(5)$ model predicts a high GUT scale $M_{\text{GUT}} > 10^{16}$ GeV. We also investigated the restrictions on the M_{B-L} scale which is associated with the $U(1)_\chi$ breaking scale. We found that the M_{B-L} scale can vary in a broad region with negligible or little effect on the value of M_{GUT} . Proton decay in this model is induced by dimension-6 operators only. The dimension-5 operator induced by SUSY contribution is suppressed due to the missing partner mechanism. We found that the partial decay width $p \rightarrow \pi^0 e^+$ is high suppressed, being at least one order of magnitude lower than the future Hyper-K sensitivity. We also studied fermion (including neutrino) masses and mixings which can also influence proton decay. We presented two scenarios of flavour textures to check the consistency of the results with fermion masses and mixing. The $B - L$ gauge breaking leads to the generation of cosmic strings. The $B - L$ scale here is not constrained by gauge coupling unification. If this scale is very close that of GUT breaking, strings can be unstable due to the decay to monopole-antimonopole pair. Such metastable strings can be used to explain the NANOGrav signals of stochastic gravitational wave background, which may be interpreted here as resulting from the decay of metastable cosmic strings.

¹E-mail: king@soton.ac.uk

²E-mail: leonta@uoι.gr

³E-mail: zhouyeling@ucas.ac.cn

1 Introduction

For more than half a century, since Georgi and Glashow proposed $SU(5)$ [1], numerous Grand Unified Theories (GUTs) have been constructed with the goal of reproducing the stupendous success of the standard model and, at the same time, providing new testable (falsifiable) predictions for particle physics and cosmology. In the years that followed, several new experimental facilities were conceived and built to verifying or disproving predictions, and imposing bounds on various exotic processes such as proton decay, and flavour changing reactions. Furthermore, accumulating cosmological data, and in particular the recent announcements of pulsar timing array (PTA) experiments such as the NANOGrav [2], EPTA [3], PPTA [4] and CPTA [5] collaborations, providing strong evidence of low frequency stochastic gravitational background can find interpretations through decays of cosmic strings [6] whose creation and subsequent evolution are intertwined with the symmetry breaking scales of novel $U(1)$'s and GUTs in general.

Among the most promising unified theories which have been proposed to embed the Standard Model is the $SU(5) \times U(1)_\chi$, the so called flipped $SU(5)$ [7, 8], where the hypercharge generator is a linear combination of the $U(1) \in SU(5)$ and $U(1)_\chi$. In contrast to the Georgi-Glashow $SU(5)$, spontaneous symmetry breaking in flipped $SU(5)$ requires only a Higgs pair of fundamentals $\mathbf{10} + \bar{\mathbf{10}}$, and thus, it dispenses with the use of the Higgs adjoint (i.e., $\mathbf{24} \in SU(5)$) representation. Although this is not a unified gauge model per se, yet it is a subgroup of the unified $SO(10)$ GUT and, as such, it possesses a number of interesting features that make it quite compelling. In string theory, for example, mechanisms such as Wilson lines or fluxes can be implemented for the $SO(10)$ GUT symmetry breaking, so that the effective theory particle spectrum is essentially described by the flipped $SU(5)$ model. Moreover, its supersymmetric (SUSY) version has been one of the few admissible candidates in particular heterotic string and F-theory constructions which do not provide adjoint or larger Higgs representations to trigger the spontaneous symmetry breaking. Flipped $SU(5)$ is also attractive since the unwanted colour triplets which accompany the Higgs doublets of GUT models, can more easily be given large masses via the missing partner mechanism. This has the additional benefit of suppressing all dimension-5 operators contributing to baryon violating processes. Thus, proton decay proceeds mainly through dimension-6 operators, with only a smaller number of operators contributing thereby suppressing the proton decay rate. Recently we have studied flipped $SU(5)$ in the framework of modular symmetry [9], focussing on the origin of fermion masses, mixing and hierarchies, including the neutrino spectrum which can arise from a type II seesaw mechanism. For some recent works in the literature, see e.g., [10–17].

In this paper we shall focus on the experimental tests of SUSY flipped $SU(5)$, including unification, proton decay, fermion masses and gravitational waves which arise from cosmic string loops associated with the breaking of the high energy $U(1)_{B-L}$. The study here complements previous recent studies where such testable predictions have been studied in the framework of $SO(10)$ [18–21]. Unlike the case of SUSY $SO(10)$ [18], we shall find that the proton decay rate is highly suppressed, rendering it practically unobservable in the foreseeable future. Moreover, the SUSY breaking scale and the $U(1)_{B-L}$ breaking scales are essentially free parameters in flipped $SU(5)$, allowing for a wide range of gravitational wave signatures. This freedom allows the NANOGrav data to be fitted more easily in

SUSY flipped $SU(5)$ than in SUSY $SO(10)$, for high $B-L$ breaking scales where unstable strings are possible, due to their decay into monopole-antimonopole pairs, without violating high frequency LIGO bounds. By contrast, in SUSY $SO(10)$, proton decay places a severe constraint on this scenario, requiring a split SUSY spectrum [18], which is not necessary for SUSY flipped $SU(5)$ where any SUSY spectrum is possible.

The layout of the remainder of this paper is as follows. In section 2 we present the spectrum of the model and describe the breaking pattern of the (flipped) $SU(5) \times U(1)_\chi$ symmetry which involves the sequence of scales $M_{\text{GUT}} > M_{B-L} > M_{\text{SUSY}}$. In section 3 we perform a two-loop renormalisation group analysis for the gauge couplings running from the GUT scale (assumed to be the scale where the g_3 and g_2 couplings attain a common value) down to the electroweak scale, and investigate the restrictions on the M_{B-L} scale which is associated with the $U(1)_\chi$ breaking. It is found that the M_{B-L} scale can vary in a broad region between M_{GUT} and M_{SUSY} with negligible or little effect on the value of M_{GUT} which is found to be $M_{\text{GUT}} \gtrsim 10^{16}$ GeV. Next, in section 4 we discuss proton decay. We specifically show that the predictions for the prevalent decay rate for $p \rightarrow \pi^0 e^+$ of this model is practically unobservable by future super-K experimental measurements. Moreover, in section 5 we discuss proton decay in conjunction with specific textures of the fermion mass matrices with particular emphasis on the role of the lepton mixing matrix. In section 6 we investigate the possibility of interpreting the recently reported data on stochastic gravitational wave background emissions through the decay of metastable cosmic strings produced due to spontaneous breaking of $U(1)_\chi$ at a high-scale. In section 7 we present our conclusions.

2 The framework

The Flipped $SU(5)$ model [7, 8] is based on the $SU(5) \times U(1)_\chi$ gauge symmetry. It was reconsidered as a possible superstring alternative to Georgi-Glashow $SU(5)$ due to the fact that its spontaneous breaking to SM symmetry requires only a pair of $\mathbf{10} + \overline{\mathbf{10}}$ Higgs representations and does not need any adjoint Higgs representation.

The spontaneous breaking of the flipped $SU(5)$ symmetry to the SM occurs via the following chain

$$\begin{aligned}
G_{51}^{\text{flip,S}} &\equiv SU(5) \times U(1)_\chi \times \text{SUSY} \\
&\quad (\mathbf{24}, 0) \downarrow \text{broken at } M_{\text{GUT}} \\
G_{3211}^{\text{S}} &\equiv SU(3)_c \times SU(2)_L \times U(1)_y \times U(1)_\chi \times \text{SUSY} \\
&\quad (\overline{\mathbf{10}}, -\tfrac{1}{2}) \supset (\mathbf{1}, \mathbf{1}, 1, -\tfrac{1}{2}) \downarrow \text{broken at } M_{B-L} \\
G_{\text{MSSM}} &\equiv SU(3)_c \times SU(2)_L \times U(1)_Y \times \text{SUSY}, \\
&\quad \downarrow \\
G_{\text{SM}} &\equiv SU(3)_c \times SU(2)_L \times U(1)_Y. \tag{1}
\end{aligned}$$

For abbreviation, we denote the lowest and the second lowest symmetry above the symmetry of the minimal supersymmetric model $G_{\text{MSSM}} \equiv SU(3)_c \times SU(2)_L \times U(1)_Y \times \text{SUSY}$

as G_{3211}^S and $G_{51}^{\text{flip},S}$, where the superscript S means the SUSY is conserved. In the symmetry G_{3211}^S , the mixing of two $U(1)$ symmetries is just a re-organisation of $U(1)_Y$ and $U(1)_{B-L}$, $U(1)_y \times U(1)_\chi \simeq U(1)_Y \times U(1)_{B-L}$. The hypercharge Y and the gauged $B-L$ number are both linear combinations of the y and χ ,

$$\begin{aligned} Y &= -\frac{1}{5}(y + 2\chi) , \\ B-L &= \frac{2}{5}(2y - \chi) . \end{aligned} \quad (2)$$

We denote scales for G_{3211}^S breaking (essentially the $U(1)_{B-L}$ breaking) and $G_{51}^{\text{flip},S}$ breaking (essentially the $SU(5)$ breaking) as M_{B-L} and M_{GUT} , respectively. Representations of Higgs multiplets achieving the breaking are given on the left hand side of the arrow. The spontaneous breaking of $G_{51}^{\text{flip},S} \rightarrow G_{3211}^S$ is achieved via a **24**-plet of $SU(5)$ which is neutral in $U(1)_\chi$. This multiplet includes a trivial singlet of G_{3211}^S . It gains a non-zero VEV, leading to the breaking of $SU(5) \rightarrow SU(3)_c \times SU(2)_L \times U(1)_y$. The breaking of $U(1)_{B-L}$ is achieved by a $(\mathbf{\bar{10}}, -\frac{1}{2})$ of $SU(5) \times U(1)_\chi$ which includes a colour- and electroweak-singlet scalar with charges 1 and $-\frac{1}{2}$ in $U(1)_y$ and $U(1)_\chi$, respectively, charge 1 in $U(1)_{B-L}$, and neutral in $U(1)_Y$.

The particle content is shown in Table 1. Here, we included particles by following the economical hypothesis that only a minimal content is included to be consistent with the SM and neutrino masses, and to achieve the symmetry breaking. In the fermion sector, only the SM fermions and right-handed neutrinos will be considered, all arranged as **10**, $\mathbf{\bar{5}}$ and **1** of $SU(5)$. In the Higgs sector, only those Higgses used to generate fermion masses and achieve the GUT symmetry breaking will be presented.

	Multiplet	Role in the model
Fermions	$(\mathbf{10}, -\frac{1}{2})$	Decomposed to Q, d^c, ν^c
	$(\mathbf{\bar{5}}, +\frac{3}{2})$	Decomposed to u^c and L
	$(\mathbf{1}, -\frac{5}{2})$	Identical to e^c
Higgs	$(\mathbf{\bar{5}}, +1)$	Generating Dirac masses for fermions
	$(\mathbf{\bar{10}}, +\frac{1}{2})$	Generating ν^c mass and triggers $U(1)_{B-L}$ breaking
	$(\mathbf{\bar{5}}, -1)$	For anomaly free
	$(\mathbf{10}, -\frac{1}{2})$	For anomaly free
	$(\mathbf{24}, 0)$	triggers the breaking of $SU(5)$

Table 1: The $SO(10)$ representations of the fields (including matter and Higgses) of our $SO(10)$ GUT model and their roles.

The **24**-plet Higgs⁴ in the last row of Table 1 is decomposed to the subgroup $SU(3)_c \times SU(2)_L \times U(1)_y \times U(1)_\chi$ in the following way,

$$(\mathbf{24}, 0) \rightarrow (\mathbf{\bar{3}}, \mathbf{2}, \frac{5}{6}, 0) + (\mathbf{3}, \mathbf{2}, -\frac{5}{6}, 0) + (\mathbf{8}, \mathbf{1}, 0, 0) + (\mathbf{1}, \mathbf{3}, 0, 0) + (\mathbf{1}, \mathbf{1}, 0, 0) \quad (3)$$

⁴As an adjoint representation, it could be replaced by a Wilson line which appears as a **24**-plet of $SU(5)$. Below the scale of $SU(5)$ breaking, either the Higgs or a Wilson line appears a VEV, and thus, there is no difference when discussing phenomenological issues below the GUT scale.

It includes a trivial singlet of the subgroup. Thus, a non-vanishing VEV along the direction of $(\mathbf{1}, \mathbf{1}, 0, 0)$ can break $G_{51}^{\text{flip}, S}$ to G_{3211}^S . This VEV alignment is achieved similarly to that in the unflipped SUSY $SU(5)$ model, with superpotential shown in [22].

The representations containing the SM matter fields, following the breaking chain $SU(5) \times U(1)_\chi \rightarrow SU(3)_c \times SU(2)_L \times U(1)_y \times U(1)_\chi \rightarrow SU(3)_c \times SU(2)_L \times U(1)_Y$ (without considering SUSY), are decomposed as

$$\begin{aligned}
(\mathbf{10}, -\frac{1}{2}) &\rightarrow (\mathbf{3}, \mathbf{2}, \frac{1}{6}, -\frac{1}{2}) + (\bar{\mathbf{3}}, \mathbf{1}, -\frac{2}{3}, -\frac{1}{2}) + (\mathbf{1}, \mathbf{1}, 1, -\frac{1}{2}), \\
&\rightarrow (\mathbf{3}, \mathbf{2}, \frac{1}{6}) + (\bar{\mathbf{3}}, \mathbf{1}, \frac{1}{3}) + (\mathbf{1}, \mathbf{1}, 0) = Q + d^c + \nu^c \\
(\bar{\mathbf{5}}, +\frac{3}{2}) &\rightarrow (\bar{\mathbf{3}}, \mathbf{1}, \frac{1}{3}, \frac{3}{2}) + (\mathbf{1}, \mathbf{2}, -\frac{1}{2}, \frac{3}{2}) \rightarrow (\bar{\mathbf{3}}, \mathbf{1}, -\frac{2}{3}) + (\mathbf{1}, \mathbf{2}, -\frac{1}{2}) = u^c + L, \\
(\mathbf{1}, -\frac{5}{2}) &\rightarrow (\mathbf{1}, \mathbf{1}, 0, -\frac{5}{2}) \rightarrow (\mathbf{1}, \mathbf{1}, 1) = e^c,
\end{aligned} \tag{4}$$

where $Q = (u, d)$ and $L = (\nu, e)$. The Higgs representations are decomposed as follows

$$\begin{aligned}
(\mathbf{5}, +1) &\rightarrow (\mathbf{3}, \mathbf{1}, -\frac{1}{3}, 1) + (\mathbf{1}, \mathbf{2}, \frac{1}{2}, 1) \rightarrow (\mathbf{3}, \mathbf{1}, -\frac{1}{3}) + (\mathbf{1}, \mathbf{2}, -\frac{1}{2}) = D + h_{\text{SM}} \\
(\bar{\mathbf{10}}, +\frac{1}{2}) &\rightarrow (\bar{\mathbf{3}}, \mathbf{2}, -\frac{1}{6}, \frac{1}{2}) + (\mathbf{3}, \mathbf{1}, \frac{2}{3}, \frac{1}{2}) + (\mathbf{1}, \mathbf{1}, -1, \frac{1}{2}), \\
&\rightarrow (\mathbf{3}, \mathbf{2}, \frac{1}{6}) + (\bar{\mathbf{3}}, \mathbf{1}, \frac{1}{3}) + (\mathbf{1}, \mathbf{1}, 0) = \bar{Q}_H + \bar{d}_H^c + \bar{\nu}_H^c,
\end{aligned} \tag{6}$$

where, h_{SM} is the SM EW-doublet Higgs, D is a heavy triplet Higgs, and $\bar{\nu}_H^c$ is the scalar whose VEV breaks $U(1)_y \times U(1)_\chi$ to $U(1)_Y$ and gives masses to the RH neutrinos. All chiral fermions are shown in the left-handed convention. In the supersymmetric case, the Higgs sector -in addition to (5) and (6)- includes also the representations $(\bar{\mathbf{5}}, -1)$ and $(\mathbf{10}, -1/2)$. In this case, for later convenience we shall use the notation $H \equiv (\mathbf{10}, -1/2)$, and $\bar{H} \equiv (\bar{\mathbf{10}}, 1/2)$. Moreover, for the fermion generations we will adopt the symbols $F_i \equiv (\mathbf{10}, -\frac{1}{2})_i$, $\bar{f}_j = (\bar{\mathbf{5}}, 3/2)_j$ where i, j are fermion generation indices. Notice also that in flipped $SU(5)$ the MSSM Higgs doublets h_d and h_u reside in $h = (\mathbf{5}, 1)$ and $\bar{h} = (\bar{\mathbf{5}}, -1)$ representations respectively.

The flipped $SU(5)$ is also regarded as a symmetry breaking pattern of the $SO(10)$ gauge group, alternative to the Georgi-Glashow $SU(5)$ or the Pati-Salam chain. Representations of fields in the group $SU(5) \times U(1)_\chi$ are achieved following the decomposition of representations of $SO(10) \rightarrow SU(5) \times U(1)_\chi$,

$$\begin{aligned}
\mathbf{16} &\rightarrow (\mathbf{10}, -\frac{1}{2}) + (\bar{\mathbf{5}}, \frac{3}{2}) + (\mathbf{1}, -\frac{5}{2}), \\
\mathbf{10} &\rightarrow (\mathbf{5}, 1) + (\bar{\mathbf{5}}, -1).
\end{aligned} \tag{7}$$

The fermion masses arise from the following $SU(5) \times U(1)_\chi$ invariant couplings

$$\begin{aligned}
\mathcal{W}_d &= (Y_d)_{ij}^* (\mathbf{10}, -\frac{1}{2})_i \cdot (\mathbf{10}, -\frac{1}{2})_j \cdot (\mathbf{5}, 1) \rightarrow (Y_d)_{ij}^* Q_i d_j^c h_d, \\
\mathcal{W}_u &= (Y_u)_{ij}^* (\mathbf{10}, -\frac{1}{2})_i \cdot (\bar{\mathbf{5}}, \frac{3}{2})_j \cdot (\bar{\mathbf{5}}, -1) \rightarrow (Y_u)_{ij}^* [Q_i u_j^c + \nu_i^c L_j] h_u,
\end{aligned}$$

$$\mathcal{W}_l = (Y_l)_{ij}^* (\mathbf{1}, -\frac{5}{2})_j \cdot (\bar{\mathbf{5}}, \frac{3}{2})_i \cdot (\mathbf{5}, 1) \rightarrow (Y_l)_{ij}^* e_j^c L_i h_d. \quad (8)$$

Here Y_u , Y_d and Y_l are 3×3 Yukawa matrices and Y_d is symmetric. These coefficient matrices are introduced with a complex conjugation to match with the SM left-right non-SUSY convention. The Dirac Yukawa coupling matrix Y_ν is read from the above equation as $Y_\nu = Y_u^T$. Also, a higher order term providing Majorana masses for the right-handed neutrinos can be written

$$\mathcal{W}_{\nu^c} = (\lambda^{\nu^c})_{ij}^* \frac{1}{2M_S} \bar{H} \bar{H} F_i F_j \rightarrow \frac{1}{2} (M_{\nu^c})_{ij}^* \nu_i^c \nu_j^c. \quad (9)$$

where $(M_{\nu^c})_{ij} = (\lambda^{\nu^c})_{ij} \frac{\langle \bar{\nu}_H^c \rangle^2}{M_S}$. The light neutrinos gain masses via the usual type-I seesaw mechanism,

$$M_\nu = -Y_\nu M_{\nu^c}^{-1} Y_\nu^T \langle h_u \rangle^2. \quad (10)$$

If additional singlet fields ν_S, Φ_i are present (which is the usual case in string derived models), then -depending on their specific properties- the following couplings could be generated

$$F \bar{H} \nu_S + \bar{h} h \Phi_i + \lambda_{ijk} \Phi_i \Phi_j \Phi_k + \dots \quad (11)$$

In addition to SM representations, the Higgs sector contains dangerous colour triplets $D_h, \bar{D}_H + c.c.$. They become massive through the following terms

$$H H h + \bar{H} \bar{H} \bar{h} \rightarrow \langle \nu_H^c \rangle D_H^c D_h + \langle \bar{\nu}_H^c \rangle \bar{D}_H^c \bar{D}_h. \quad (12)$$

Note that, if no other symmetry exists the terms such as $H F_i h, H \bar{f}_j \bar{h}$ could be possible. Such terms would generate dangerous mixing between Higgs and Matter fields:

$$(aF + bH) \bar{f}_j h + \dots \quad (13)$$

Remarkably, a softly broken Z_2 symmetry [23] which is odd only for the Higgs field $H \rightarrow -H$, suppresses all these couplings from the Lagrangian, while all the previous (useful) terms are left intact.⁵ Similar symmetries have been discussed in [24].

For rank-one mass textures the couplings in Eq. (8) predict $m_t = m_{\nu_\tau}$ at the GUT scale. However, in contrast to the standard $SU(5)$ model, down quark and lepton mass matrices are not related, since at the $SU(5) \times U(1)_\chi$ level they originate from different Yukawa couplings. This is an important difference with the ordinary $SU(5)$. We know that in order to obtain the observed lepton and down quark mass spectrum at low energies, at the GUT scale the following relations should hold [25]

$$m_\tau = m_b, \quad m_\mu = 3 m_s. \quad (14)$$

In the ordinary $SU(5)$, the masses are related and the relations can be attributed to the Higgs adjoint which couples differently. This mechanism though is not operative in the

⁵This Z_2 must be softly broken to avoid the domain wall problem after the spontaneous breaking of Z_2 once H gains the VEV.

minimal flipped $SU(5)$ due to the absence of the adjoint, as noticed above, thus the mass matrices are not related and Yukawas should be adjusted accordingly.

We further review the derivation of the matching condition between gauge couplings of $U(1)_Y$ and those of $SU(5) \times U(1)_\chi$. Computing the traces and finding normalisation constants so that the final trace is 2, give:

$$\begin{aligned} C_y^2 y^2 &= C_y^2 \frac{10}{3} = 2 \rightarrow C_y = \sqrt{\frac{3}{5}}, \\ C_\chi^2 \chi^2 &= C_\chi^2 20 = 2 \rightarrow C_\chi = \frac{1}{\sqrt{10}}. \end{aligned} \quad (15)$$

In terms of normalised generators, the hypercharge is written as $Y = \frac{1}{5C_y} (\tilde{y} + \kappa \tilde{\chi})$, where the ratio is $\kappa \equiv 2 \frac{C_y}{C_\chi} = 2\sqrt{6}$. Finally $\tilde{Y} = \sqrt{\frac{3}{5}} Y$ implies

$$\tilde{Y} = \frac{1}{5} (\tilde{y} + 2\sqrt{6} \tilde{\chi}) , \quad (16)$$

and for the $U(1)_Y$ gauge coupling

$$(1 + \kappa^2) \frac{1}{a_Y} = \frac{1}{a_5} + \kappa^2 \frac{1}{a_\chi} \quad (17)$$

or equivalently,

$$\frac{1}{\alpha_{\tilde{Y}}} = \frac{1}{25} \frac{1}{\alpha_{\tilde{y}}} + \frac{24}{25} \frac{1}{\alpha_{\tilde{\chi}}} . \quad (18)$$

For initial values $a_\chi = a_5$, we obtain the standard relation of $SU(5)$. In general, however, $a_\chi \neq a_5$, and there is more flexibility.

3 Two-loop RG running

Renormalisation group (RG) running of the gauge couplings can be briefly described in the follow picture. As the energy scale Q runs from one intermediate symmetry breaking scale to its neighbouring intermediate symmetry breaking scale (e.g., from M_{B-L} to M_{GUT}), the gauge coupling varies continuously along with Q . For energy scale jumps across the intermediate symmetry breaking scale (e.g., M_{B-L}), gauge couplings below and above the scale satisfy matching conditions.

Given a gauge symmetry $G \equiv H_1 \times \cdots \times H_n$ as a product of simple Lie groups H_i for $i = 1, 2, \cdots$ between two neighbouring symmetry breaking scales Q_1 and Q_2 , the two-loop RG equation of the gauge coupling g_i for the group H_i is given by

$$\frac{d\alpha_i}{dt} = \beta_i(\alpha_i) , \quad (19)$$

where $\alpha_i = g_i^2/(4\pi)$, $t = \log(Q/Q_0)$ is the logarithm of the energy scale Q for $Q_1 < Q < Q_2$, and Q_0 is an arbitrary energy scale here fixed at the Z pole mass. The β function on

Model	Matter (Super-)Fields	Higgs (Super-)Fields
$G_{51}^{\text{flip,S}}$	$(\mathbf{10}, -\frac{1}{2}) + (\bar{\mathbf{5}}, +\frac{3}{2}) + (\mathbf{1}, -\frac{5}{2})$	$(\mathbf{5}, +1) + (\bar{\mathbf{10}}, +\frac{1}{2})$
G_{3211}^S	$(\mathbf{3}, \mathbf{2}, \frac{1}{6}, -\frac{1}{2}) + (\bar{\mathbf{3}}, \mathbf{1}, -\frac{2}{3}, -\frac{1}{2}) + (\mathbf{1}, \mathbf{1}, 1, -\frac{1}{2})$ $+ (\bar{\mathbf{3}}, \mathbf{1}, \frac{1}{3}, \frac{3}{2}) + (\mathbf{1}, \mathbf{2}, -\frac{1}{2}, \frac{3}{2}) + (\mathbf{1}, \mathbf{1}, 0, -\frac{5}{2})$	$(\mathbf{1}, \mathbf{2}, \frac{1}{2}, 1) + (\mathbf{1}, \mathbf{2}, -\frac{1}{2}, -1)$ $+ (\mathbf{1}, \mathbf{1}, -1, \frac{1}{2}) + (\mathbf{1}, \mathbf{1}, 1, -\frac{1}{2})$
G_{MSSM}	$(\mathbf{3}, \mathbf{2}, \frac{1}{6}) + (\bar{\mathbf{3}}, \mathbf{1}, \frac{1}{3}) + (\mathbf{1}, \mathbf{1}, 0)$ $(\bar{\mathbf{3}}, \mathbf{1}, -\frac{2}{3}) + (\mathbf{1}, \mathbf{2}, -\frac{1}{2}) + (\mathbf{1}, \mathbf{1}, 1)$	$(\mathbf{1}, \mathbf{2}, -\frac{1}{2}) + (\mathbf{1}, \mathbf{2}, \frac{1}{2})$
G_{SM}	$(\mathbf{3}, \mathbf{2}, \frac{1}{6}) + (\bar{\mathbf{3}}, \mathbf{1}, \frac{1}{3}) + (\mathbf{1}, \mathbf{1}, 0)$ $(\bar{\mathbf{3}}, \mathbf{1}, -\frac{2}{3}) + (\mathbf{1}, \mathbf{2}, -\frac{1}{2}) + (\mathbf{1}, \mathbf{1}, 1)$	$(\mathbf{1}, \mathbf{2}, \frac{1}{2})$

Table 2: Decomposition of the matter multiplet **16** and Higgses in each step of the breaking chain. Note that the adjoint **24** Wilson line is not included in the table as it is not a field.

the right hand side is written as

$$\beta_i = -\frac{1}{2\pi}\alpha_i^2(b_i + \frac{1}{4\pi}\sum_j b_{ij}\alpha_j) , \quad (20)$$

up to the two-loop level. Here, b_i and b_{ij} are the normalised coefficients of one- and two-loop contributions of fields (or superfields), respectively. Both are determined by the group H_i and representations of particles in H_i , and b_{ij} further depend on the particle representation in H_j . In this work, we will simply list their values when they are used for given particle contents in our model, which are given in Table 2. For each energy-scale interval from the EW scale to the scale of flipped $SU(5)$ breaking in this table, the beta coefficients b_i and b_{ij} are given in Table 3. These coefficients are calculated in the following way. For example, for RG running from G_{MSSM} down to G_{SM} , b_i and b_{ij} are calculated by including only fields preserving G_{SM} in Table 2. We refer to [20] for more general discussions on how to calculate these coefficients. The above differential equation has analytical solution

$$\alpha_i^{-1}(t) = \alpha_i^{-1}(t_1) - \frac{b_i}{2\pi}(t - t_1) + \sum_j \frac{b_{ij}}{4\pi b_i} \log \left(1 - \frac{b_j}{2\pi} \alpha_j(t_1) (t - t_1) \right) , \quad (21)$$

if the condition $b_j \alpha_j |t_2 - t_1| < 1$ is satisfied and no particle decouples for t varying from t_1 to t_2 [26].

During a symmetry breaking at a certain scale (e.g., M_{GUT} , M_{B-L} or M_{SUSY}), the gauge couplings of the larger symmetry and those of the residual symmetry after the symmetry breaking satisfy matching conditions. Below we list one-loop matching conditions which appear in the GUT breaking chains. In this work, we are encountering two types of symmetry breaking: 1) at M_{B-L} and M_{GUT} , the gauge symmetry breaking, where M_{B-L} and M_{GUT} are identified as corresponding gauge boson masses; 2) at M_{SUSY} , the SUSY breaking, where we assume a unified mass scale for all superpartners and this scale is recognised as M_{SUSY} .⁶ Matching conditions at the scale of gauge symmetry breaking are

⁶A unified mass scale for all SUSY particles at M_{SUSY} should be considered as a rough assumption here. In SUSY GUTs, a dark matter candidate is identified with the lightest SUSY particle provided it

$G_{51}^{\text{flip,S}}$	broken at $Q = M_{\text{GUT}}$
\downarrow	$\{b_i\} = \begin{pmatrix} -3 \\ 1 \\ \frac{39}{5} \\ \frac{129}{20} \end{pmatrix}, \quad \{b_{ij}\} = \begin{pmatrix} 14 & 9 & \frac{11}{5} & \frac{9}{5} \\ 24 & 25 & \frac{9}{5} & \frac{11}{5} \\ \frac{88}{5} & \frac{27}{5} & \frac{271}{25} & \frac{54}{25} \\ \frac{72}{5} & \frac{33}{5} & \frac{54}{25} & \frac{1593}{200} \end{pmatrix}$
G_{3211}^{S}	broken at $Q = M_{B-L}$
\downarrow	$\{b_i\} = \begin{pmatrix} -3 \\ 1 \\ \frac{33}{5} \end{pmatrix}, \quad \{b_{ij}\} = \begin{pmatrix} 14 & 9 & \frac{11}{5} \\ 24 & 25 & \frac{9}{5} \\ \frac{88}{5} & \frac{27}{5} & \frac{199}{25} \end{pmatrix}$
G_{MSSM}	broken at $Q = M_{\text{SUSY}}$
\downarrow	$\{b_i\} = \begin{pmatrix} -7 \\ -\frac{19}{6} \\ \frac{41}{10} \end{pmatrix}, \quad \{b_{ij}\} = \begin{pmatrix} -26 & \frac{9}{2} & \frac{11}{10} \\ 12 & \frac{35}{6} & \frac{9}{10} \\ \frac{44}{5} & \frac{17}{10} & \frac{199}{50} \end{pmatrix}$
G_{SM}	

Table 3: Coefficients b_i and b_{ij} of gauge coupling β functions appearing in the specified breaking chain.

given as follows. For a simple Lie group $SU(m)$ broken to subgroup $SU(n)$ ($m > n > 1$) at the scale $Q = M_I$, the one-loop matching condition is given by [31]

$$SU(m) \rightarrow SU(n) : \quad \alpha_{SU(m)}^{-1}(M_I) - \frac{m}{12\pi} = \alpha_{SU(n)}^{-1}(M_I) - \frac{n}{12\pi}, \quad (22)$$

where the quadratic Casimir for the adjoint presentation of the $SU(n)$ group, $C_2(SU(n)) = n$, has been used. For $G_{3211}^{\text{S}} \rightarrow G_{\text{SM}}$, we encounter the breaking, $U(1)_y \times U(1)_\chi \rightarrow U(1)_Y$, which has the matching condition:

$$\frac{1}{25}\alpha_y^{-1}(M_{B-L}) + \frac{24}{25}\alpha_{\tilde{\chi}}^{-1}(M_{B-L}) = \alpha_Y^{-1}(M_{B-L}). \quad (23)$$

The matching condition at the SUSY breaking scale M_{SUSY} is induced by the usage of different renormalisation schemes for the scale below and above M_{SUSY} . At $Q < M_{\text{SUSY}}$, the RGE was derived in the usual $\overline{\text{MS}}$ scheme. At $Q > M_{\text{SUSY}}$, it was calculated in the $\overline{\text{DR}}$ scheme, where SUSY can be preserved [32]. The relation of couplings in the two schemes is described by

$$\alpha_{\text{DR}}^{-1} = \alpha_{\text{MS}}^{-1} - \frac{1}{12\pi}C_2(H_i), \quad (24)$$

where H_i is a Lie group. For $H_i = U(1)$, $C_2(U(1)) = 0$, whilst $C_2(SU(n))$ has been given above.

At the EW scale, we set the SM gauge couplings at their best-fit values, i.e., $\alpha_3 = 0.1184$, $\alpha_2 = 0.033819$ and $\alpha_1 = 0.010168$ [33]. Applying the matching conditions at intermediate

is neutral [27, 28]. Restriction on the dark matter overproduction sets an upper bound around 10 TeV on the dark matter mass [29], and also on the SUSY scale. By splitting the mass spectrum of SUSY particles, e.g., that in the split SUSY [30], the SUSY scale is relaxed and in general can be treated as a free parameter varying up to the GUT scale. Note that splitting the mass spectrum slightly modifies the β coefficients b_i and b_{ij} at scale lower than M_{SUSY} ; seeing e.g., our recent discussion in [18]. Its influence on the RG running behaviour of the gauge couplings is small and goes beyond the main point of this paper.

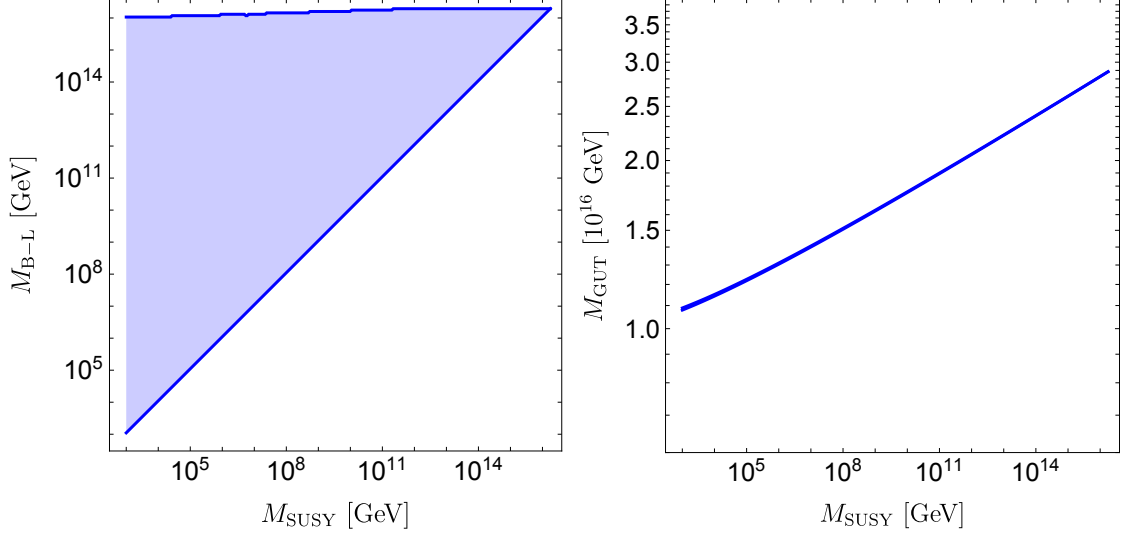


Figure 1: Mass scales restricted by gauge unification in SUSY $SU(5)$ with $1 \text{ TeV} < M_{\text{SUSY}} < M_{B-L} < M_{\text{GUT}}$.

scales and running RGEs in the interval between each two scales nearby, gauge couplings can run from the EW scale to a sufficient high scale.

In the flipped $SU(5)$ framework, gauge couplings of $SU(3)_c$, $SU(2)_L$ and $U(1)_y$ are supposed to be unified into a single gauge coupling, i.e., g_5 with $\alpha_5 \equiv g_5^2/4\pi$ satisfying

$$\alpha_3^{-1}(M_{\text{GUT}}) - \frac{3}{12\pi} = \alpha_2^{-1}(M_{\text{GUT}}) - \frac{2}{12\pi} = \alpha_{\tilde{y}}^{-1}(M_{\text{GUT}}) \quad (25)$$

Some interesting features of correlations of M_{SUSY} , M_{B-L} and M_{GUT} and the gauge couplings g_y and $g_{\tilde{\chi}}$ can be summarised below.

- As seen in table 3, the β -coefficients b_i and b_{ij} for $SU(3)_c \times SU(2)_L$ do not change for the scale passing M_{B-L} . Thus M_{B-L} does not influence the unification of $SU(3)_c \times SU(2)_L \subset SU(5)$ at M_{GUT} , and thus M_{GUT} is only correlated with M_{SUSY} .
- g_y is correlated with M_{B-L} and M_{GUT} via the second identity of Eq. (25), and accordingly, $g_{\tilde{\chi}}$ is correlated with these scales via Eq. (23). It is also convenient to obtain correlation between g_{B-L} and these scale via the matching condition

$$\alpha_{B-L}^{-1} = \frac{8}{3} \left(\frac{2}{5} \alpha_{\tilde{y}}^{-1} + \frac{3}{5} \alpha_{\tilde{\chi}}^{-1} \right), \quad (26)$$

where $\alpha_{B-L} = g_{B-L}^2/(4\pi)$ is the usual unnormalised coupling as the factor $8/3$ in the right hand side appears.

Eventually, the unification leaves only two free parameters among scales and gauge couplings. One can choose, e.g., M_{B-L} and M_{GUT} , as variables to determine the rest of the parameters.

The above RG running procedure involves three energy scales M_{MSSM} , M_{B-L} and M_{GUT} . Gauge unification requires that two SM gauge couplings g_3 and g_2 meet at M_{GUT} , which

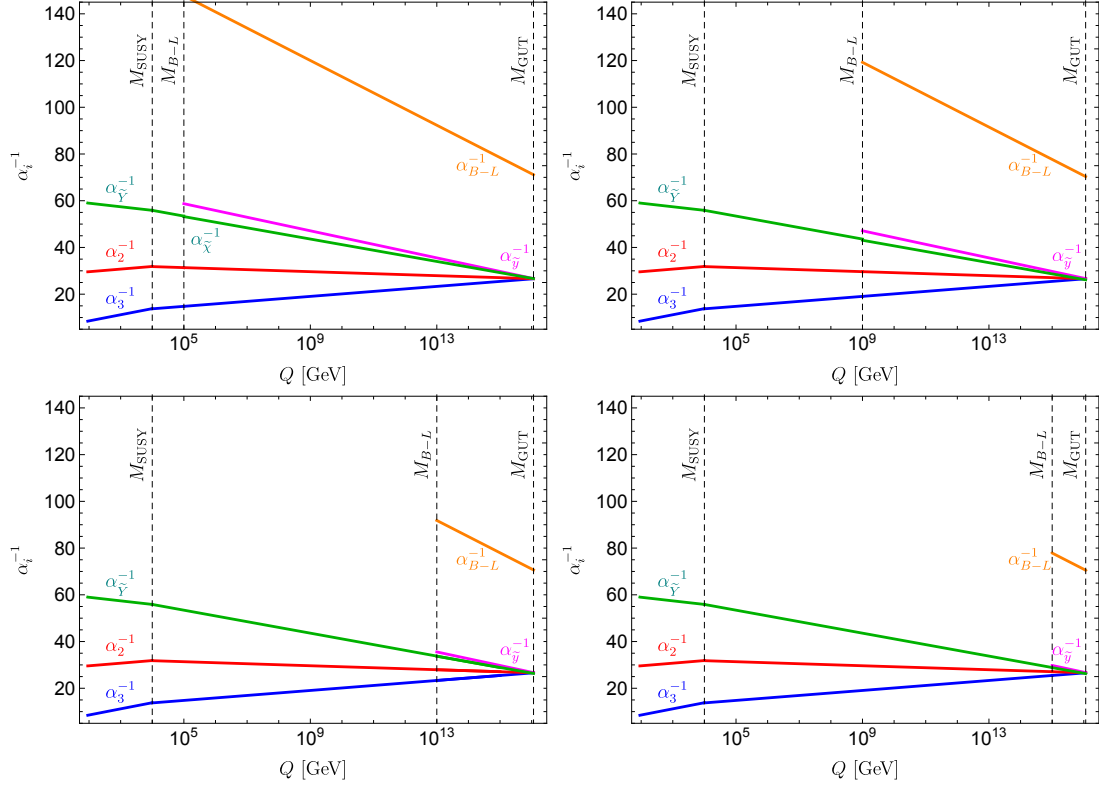


Figure 2: Gauge couplings running with the scale. From the top left to the bottom right, $M_{B-L} = 10^5, 10^9, 10^{13}, 10^{15}$ GeV are used and $M_{\text{SUSY}} = 10$ TeV is fixed. Note that these values are used only for illustration purposes as some of them are not consistent with neutrino mass as will be discussed in section 5. The $SU(5)$ unification scale M_{GUT} is solved via the unification of α_2 and α_3 . In the range $M_{B-L} < Q < M_{\text{GUT}}$, we show the running of the unnormalised coupling α_{B-L} as the $U(1)_{B-L}$ symmetry is essential to neutrino mass and the generation of cosmic strings.

is different from the situation in usual non-flipped $SU(5)$ or $SO(10)$ models that all three SM gauge couplings meet at the GUT scale, up to matching conditions. Furthermore, note that the inclusion of the intermediate scale M_{B-L} does not change the beta coefficients in the $SU(3)_c \times SU(2)_L$ block, as seen in Table 3. As a consequence, M_{B-L} has little influence on the RG running of g_3 and g_2 , and thus is not correlated to the unification scale M_{GUT} except the requirement $M_{\text{GUT}} \geq M_{B-L}$. The allowed parameter space for three energy scales are shown in Fig. 1, where $1 \text{ TeV} \leq M_{\text{SUSY}} \leq M_{B-L} \leq M_{\text{GUT}}$ is assumed.

Cases of gauge coupling RG running with the energy scale is shown in Fig 2, where $M_{\text{SUSY}} = 10$ TeV is fixed and $M_{B-L} = 10^4, 10^9, 10^{13}, 10^{15}$ GeV are used from the top left to the bottom right panels for illustration. The GUT scale M_{GUT} , referring to the breaking of $SU(5)$, is determined by the unification of α_2 and α_3 . It is seen that varying the scale M_{B-L} does not influence the unification scale M_{GUT} . We also show the RG running of the coupling α_{B-L} between M_{B-L} and M_{GUT} . Setting $M_{B-L} = 10^{15}$ GeV leads to the gauge coupling $g_{B-L} = \sqrt{4\pi/\alpha_{B-L}^{-1}} = 0.40$. Assuming a lower $B-L$ breaking scale could predict a slightly smaller g_{B-L} value. For example, $M_{B-L} = 10^5$ GeV leads to $g_{B-L} = 0.29$.

4 Proton decay

We discuss the proton decay in the SUSY flipped $SU(5)$ model. Heavy gauge bosons are integrated out at low energy and leave dimension-6 operators. These 4-Fermi interactions violate the baryon number and lead to the decay of nucleons. A typical channel is $p \rightarrow \pi^0 e^+$. In the SUSY extension, dimension-5 between two fermions and two superpartners, mediated by colour-triplet Higgs, is another source of baryon number violation. These operators get dressed via loop corrections and might enhance the decay width of another channel $p \rightarrow K^+ \bar{\nu}$ greatly. In SUSY $SU(5)$ or $SO(10)$ models, a null result for the observation of proton decay raises the SUSY breaking scale (see discussions e.g. in [34] and [35, 36]). Furthermore, careful treatment should be paid to avoid the overproduction of the dark matter, which is predicted to be the lightest supersymmetric particle if it is neutral [18]. In SUSY flipped $SU(5)$ models, as will be examined in the coming subsection, the dimension-5 contribution is suppressed due to the missing partner mechanism, thus there is no restriction on the SUSY breaking scale from proton decay. Only dimension-6 contribution need to be considered, as will be done in section 4.2.

4.1 Dimension-5 contributions

Due to the missing partner mechanism in Flipped $SU(5)$ the dimension-5 operators are suppressed and as such, they are neglected. This suppression mechanism works as follows. The extra down-type triplets, arise from the decomposition of the various Higgs representations, and in our particular assignments we have

$$d_H^c \in H, \bar{d}_H^c \in \bar{H}, D \in h, \bar{D} \in \bar{h}.$$

When $H + \bar{H}$ acquire vevs, the tree-level superpotential terms related to the triplet masses yield the following mass terms for the triplets

$$\lambda_1 H H h + \lambda_2 \bar{H} \bar{H} \bar{h} \rightarrow \lambda_1 \langle \nu_H^c \rangle d_H^c D + \lambda_2 \langle \bar{\nu}_H^c \rangle \bar{d}_H^c \bar{D}. \quad (27)$$

It can readily be observed that due to the symmetries, there are no superpotential terms which couple directly the two triplets residing in $\mathbf{10}_H, \bar{\mathbf{10}}_{\bar{H}}$ representations. It is possible however, that suppressed contributions $\sim \frac{m^{n+1}}{M_P^n} \bar{H} H$ might arise at higher (NR)-order. Furthermore, notice that a superpotential term which couples the two Higgs fiveplets $\mu \bar{\mathbf{5}}_{\bar{h}} \mathbf{5}_h$ implies a direct mass $\mu \bar{D} D$ which is suppressed compared to the GUT mass terms (27), i.e., $\mu \ll \langle \nu_H^c \rangle$. Assuming for simplicity $\lambda_1 \langle \nu_H^c \rangle = \lambda_2 \langle \bar{\nu}_H^c \rangle \equiv M_{d_H^c D}$, in the basis (D, d_H^c) we can write the triplet mass matrix as follows

$$M_T = \begin{pmatrix} \mu & m_{d_H^c D} \\ m_{d_H^c D} & m_{\bar{D} D} \end{pmatrix} \Rightarrow \begin{pmatrix} a & b \\ b & d \end{pmatrix}, \quad (28)$$

in a self-explanatory notation. Of course $b > d > a$. We assume for simplicity that all entries are real, so that we can diagonalise the mass matrix by

$$V = \begin{pmatrix} \cos \theta & \sin \theta \\ -\sin \theta & \cos \theta \end{pmatrix}.$$

Now, a tree-level diagram leading to d-5 operators mediated by D - \bar{D} implies an effective mass in the propagator

$$\frac{1}{M_{\text{eff}}^2} = \sum_{j=1}^2 V_{1j} \frac{1}{M_{T_j}^2} V_{j2}^\dagger = \frac{(a+d)b}{(ad-b^2)^2} \equiv \frac{(a+d)b}{(\text{Det} M_T)^2} \sim \frac{m_{\bar{D}D}}{m_{d_H^c D}^3}. \quad (29)$$

For the hierarchies given above, $M_{\text{eff}} \gg m_{d_H^c D} > m_{\bar{D}D}$ which implies sufficient suppression to dimension-5 operators.

4.2 Dimension-6 contributions

We are then left with dimension-6 operator contributions mediated by heavy gauge bosons. A model-independent description of dimension-6 BNV operators are given by

$$\begin{aligned} & \frac{1}{\Lambda_1^2} [(\bar{u}_R^c \gamma^\mu Q)(\bar{d}_R^c \gamma_\mu L) + (\bar{u}_R^c \gamma^\mu Q)(\bar{e}_R^c \gamma_\mu Q)] \\ & + \frac{1}{\Lambda_2^2} [(\bar{d}_R^c \gamma^\mu Q)(\bar{u}_R^c \gamma_\mu L) + (\bar{d}_R^c \gamma^\mu Q)(\bar{\nu}_R^c \gamma_\mu Q)]. \end{aligned} \quad (30)$$

Λ_1 and Λ_2 are heavy mass scales determined by the GUT model. In the usual non-flipped $SU(5)$, $\Lambda_1 = M_{\text{GUT}}/g_{\text{GUT}}$ and $\Lambda_2 \rightarrow \infty$; In flipped $SU(5)$, $\Lambda_2 = M_{\text{GUT}}/g_{\text{GUT}}$ and $\Lambda_1 \rightarrow \infty$; In $SO(10)$, $\Lambda_1 = \Lambda_2 = M_{\text{GUT}}/g_{\text{GUT}}$, where g_{GUT} and M_{GUT} should be understood as gauge couplings and heavy gauge boson masses of the relevant gauge group.

We consider dimension-6 operators contributing to the typical channel $p \rightarrow \pi^0 e^+$ in flipped $SU(5)$. As seen in Fig. 1, the lower bound of M_{GUT} , due to the requirement of gauge unification, is always larger than 10^{16} GeV, which is high enough to avoid current known experimental constraints set by Super-K, $\tau(p \rightarrow \pi^0 e^+) > 2.4 \times 10^{34}$ yr [37]. A further suppression in the flipped $SU(5)$ is the absence of the decay to a right-handed charged lepton. Since e_R is arranged as a gauge singlet in the model, there is no gauge boson mediating BNV interactions to e_R . This is seen in the second row of Eq. (30), where only the left-handed e_L is involved in the operator. As a comparison, in the unflipped $SU(5)$ or $SO(10)$, the two operators in the first row of Eq. (30) include the charged lepton, either e_L or e_R . Thus, they both contribute to the decay $p \rightarrow \pi^0 e^+$.

The lifetime referring to this channel is defined as $\tau(p \rightarrow \pi^0 e^+) = 1/\Gamma(p \rightarrow \pi^0 e^+)$ with the partial decay width

$$\Gamma(p \rightarrow \pi^0 e^+) = \frac{m_p}{32\pi} \left(1 - \frac{m_\pi^2}{m_p^2}\right)^2 \frac{g_5^4}{M_{\text{GUT}}^4} A_L^2 A_{S_1}^2 (\langle \pi^0 | (ud)_R u_L | p \rangle_e)^2 |V_{ud}|^2 |(U_l)_{11}|^2, \quad (31)$$

where $A_L = 1.247$ is the long range effect, and the short range effect

$$\begin{aligned} A_{S_1} &= \left[\frac{\alpha_3(M_{\text{SUSY}})}{\alpha_3(M_{\text{GUT}})} \right]^{\frac{4}{9}} \left[\frac{\alpha_2(M_{\text{SUSY}})}{\alpha_2(M_{\text{GUT}})} \right]^{-\frac{3}{2}} \left[\frac{\alpha_{\tilde{Y}}(M_{\text{SUSY}})}{\alpha_{\tilde{Y}}(M_{\text{GUT}})} \right]^{\frac{1}{18}} \\ &\times \left[\frac{\alpha_3(m_Z)}{\alpha_3(M_{\text{SUSY}})} \right]^{\frac{2}{7}} \left[\frac{\alpha_2(m_Z)}{\alpha_2(M_{\text{SUSY}})} \right]^{-\frac{27}{38}} \left[\frac{\alpha_{\tilde{Y}}(m_Z)}{\alpha_{\tilde{Y}}(M_{\text{SUSY}})} \right]^{-\frac{11}{82}}, \end{aligned} \quad (32)$$

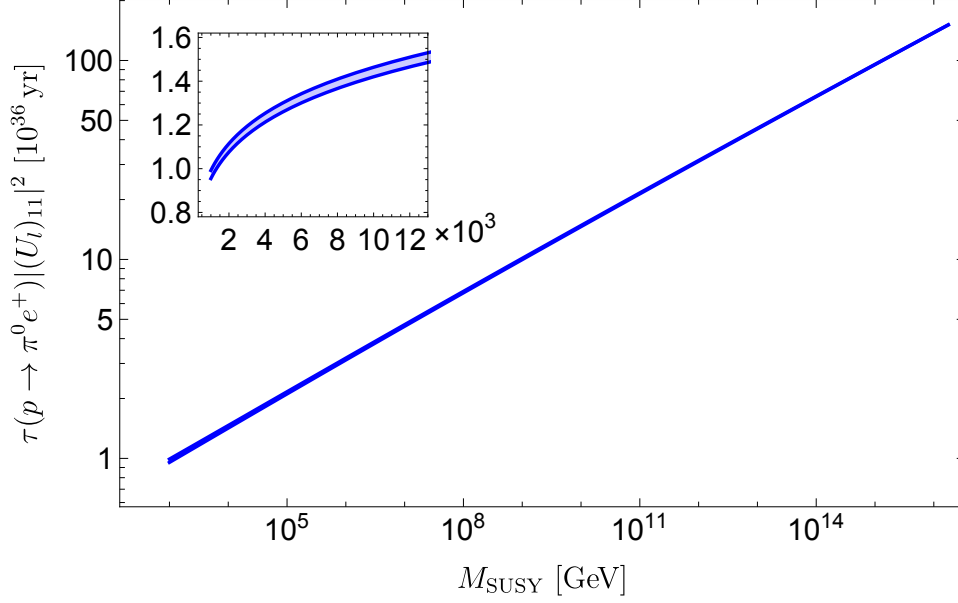


Figure 3: Prediction of partial proton lifetime via the channel $p \rightarrow \pi^0 e^+$ vs the SUSY scale.

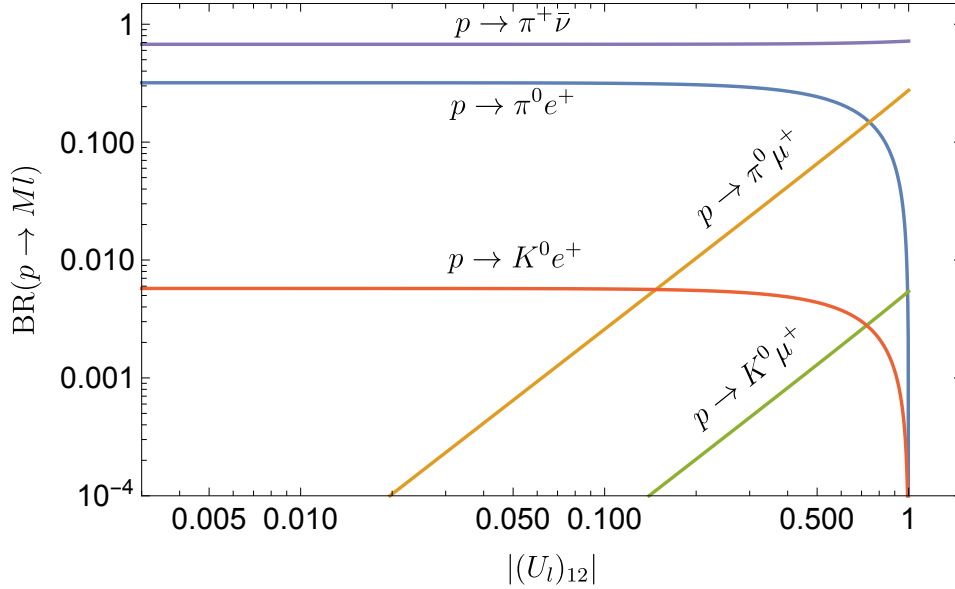


Figure 4: Branching ratios for different proton decay channels as a function of $|(U_l)_{12}|$.

depending on energy scales. $\langle \pi^0 | (ud)_R u_L | p \rangle_e = -0.131$ is the relevant hadronic matrix element appearing in the channel $p \rightarrow \pi^0 e^+$, derived via lattice simulation [38].

Taking the gauge unification in the last section into account, we have scanned all mass scales and confirmed that $\Gamma(p \rightarrow \pi^0 e^+) / |(U_l)_{11}|^2$ is no more than $[10^{36} \text{ yr}]^{-1}$, seeing in Fig. 3. This decay width is in general small enough and cannot be excluded by the future proton decay measurement including Hyper-K, unless $|(U_l)_{11}|^2 < 0.1$.

Following the formulation in [10], we list ratios of all other proton decay channels to $p \rightarrow \pi^0 e^+$ as

$$\frac{\Gamma(p \rightarrow \pi^0 \mu^+)}{\Gamma(p \rightarrow \pi^0 e^+)} = \left[\frac{\langle \pi^0 | (ud)_R u_L | p \rangle_\mu}{\langle \pi^0 | (ud)_R u_L | p \rangle_e} \right]^2 \frac{|(U_l)_{12}|^2}{|(U_l)_{11}|^2} \simeq 0.811 \frac{|(U_l)_{12}|^2}{|(U_l)_{11}|^2},$$

$$\begin{aligned}
\frac{\Gamma(p \rightarrow K^0 e^+)}{\Gamma(p \rightarrow \pi^0 e^+)} &= \left[\frac{\langle K^0 | (us)_{RuL} | p \rangle_e}{\langle \pi^0 | (ud)_{RuL} | p \rangle_e} \right]^2 \frac{|V_{us}|^2}{|V_{ud}|^2} \simeq 0.018, \\
\frac{\Gamma(p \rightarrow K^0 \mu^+)}{\Gamma(p \rightarrow \pi^0 e^+)} &= \left[\frac{\langle K^0 | (us)_{RuL} | p \rangle_\mu}{\langle \pi^0 | (ud)_{RuL} | p \rangle_e} \right]^2 \frac{|V_{us}|^2 |(U_l)_{12}|^2}{|V_{ud}|^2 |(U_l)_{11}|^2} \simeq 0.016 \frac{|(U_l)_{12}|^2}{|(U_l)_{11}|^2}, \\
\frac{\Gamma(p \rightarrow \pi^+ \bar{\nu})}{\Gamma(p \rightarrow \pi^0 e^+)} &= \left[\frac{\langle \pi^+ | (ud)_{RuL} | p \rangle}{\langle \pi^0 | (ud)_{RuL} | p \rangle_e} \right]^2 \frac{1}{|V_{ud}|^2 |(U_l)_{11}|^2} \simeq \frac{2.12}{|(U_l)_{11}|^2}. \quad (33)
\end{aligned}$$

Here, $\Gamma(p \rightarrow \pi^+ \bar{\nu})$ represents $\sum_i \Gamma(p \rightarrow \pi^+ \bar{\nu}_i)$. $p \rightarrow K^+ \bar{\nu}_i$ is not listed as it is proven to be forbidden by the unitarity of the CKM matrix [10]. On the right-hand side of the equation, all nuclear matrix element values are taken their numerical values obtained from the lattice simulation [38]. As a consequence, all ratios depend on the undetermined unitary matrix U_l . It is convenient to write out the branching ratio $\text{BR}(p \rightarrow M l) = \Gamma(p \rightarrow M l) / \Gamma_p$, where M is a meson and l is a lepton, and Γ_p is the total decay width of the proton. Considering a natural scenario $|(U_l)_{13}| \ll |(U_l)_{12}|$ and thus, $|(U_l)_{11}| \simeq \sqrt{1 - |(U_l)_{12}|^2}$. All BRs then depend only on the off-diagonal entry $|(U_l)_{12}|$. We show BRs for all channels as functions of $|(U_l)_{12}|$ in Fig. 4. It is a special feature in flipped $SU(5)$ that the BR of the anti-neutrino channel, $p \rightarrow \pi^+ \bar{\nu}$ is larger than the positron channel, as both ν_R and ν_L are involved in BNV operators. Varying $|(U_l)_{12}|$ in $(0, 1)$, we obtain the branching of this neutrino channel around 70%.

To end the section, we mention the neutron BNV decay. The dominant channel is $n \rightarrow \pi^0 \bar{\nu}$ with decay width $\Gamma(n \rightarrow \pi^0 \bar{\nu}) \simeq \frac{1}{2} \Gamma(p \rightarrow \pi^+ \bar{\nu})$, directly obtained via the isospin transformation. The neutron partial lifetime is typical at or above 10^{36} yr.

5 Flavour textures of matter fields

In this section we compute the proton decay branching ratios in two scenarios where Yukawa mass matrices are assumed in special textures. We show how the SUSY flipped $SU(5)$ matches with fermion data via these scenarios. Before the discussion, we list the mass and Yukawa properties in the flipped $SU(5)$ model. We have three free Yukawa coupling matrices Y_ν , Y_e and Y_d and one Majorana matrix M_{ν^c} , with Y_d and M_{ν^c} diagonal. The up-quark Yukawa coupling matrix is correlated with the Dirac Yukawa coupling matrix between the left- and right-handed neutrinos as $Y_u = Y_\nu^T$, and the Majorana mass matrix for light neutrinos is given by $M_\nu = -Y_\nu M_{\nu^c}^{-1} Y_\nu^T \langle h_u \rangle^2$. These matrices, can be diagonalised as $U_f^\dagger Y_f U'_f = \hat{Y}_f \equiv \text{diag}\{y_{f1}, y_{f2}, y_{f3}\}$, where $f = e, u, d$ (for $f = e$, $(y_{f1}, y_{f2}, y_{f3}) = (y_e, y_\mu, y_\tau)$, etc) and $U_\nu^\dagger M_\nu U_\nu^* = \hat{M}_\nu \equiv \text{diag}\{m_1, m_2, m_3\}$. Here, U_l is the unitary matrix contributing to the proton decay ratio in the Eq. (33). As Y_d is symmetric, $U'_d = U_d^*$ is satisfied. After the diagonalisation, we obtain the quark and lepton flavour mixing matrices as $V_{\text{CKM}} = U_u^\dagger U_d$ and $U_{\text{PMNS}} = U_l^\dagger U_\nu$. In particular, the lepton flavour mixing matrix, i.e., the PMNS matrix, up to three unphysical phases on the left hand side, is parametrised as follows

$$U_{\text{PMNS}} = P_l \begin{pmatrix} c_{12}c_{13} & s_{12}c_{13} & s_{13}e^{-i\delta} \\ -s_{12}c_{23} - c_{12}s_{13}s_{23}e^{i\delta} & c_{12}c_{23} - s_{12}s_{13}s_{23}e^{i\delta} & c_{13}s_{23} \\ s_{12}s_{23} - c_{12}s_{13}c_{23}e^{i\delta} & -c_{12}s_{23} - s_{12}s_{13}c_{23}e^{i\delta} & c_{13}c_{23} \end{pmatrix} P_\nu, \quad (34)$$

where θ_{ij} (for $ij = 12, 13, 23$) are three mixing angles, δ is the Dirac CP phase, $P_\nu = \text{diag}\{1, e^{i\alpha_{21}/2}, e^{i\alpha_{31}/2}\}$ is the Majorana phase matrix and $P_l = \text{diag}\{e^{i\beta_1}, e^{i\beta_2}, e^{i\beta_3}\}$ is a diagonal phase matrix without physical correspondence at low energy. The CKM matrix can be parameterised similarly to (34) with a 3×3 matrix in the middle, involving three mixing angles θ_{ij}^q and a Dirac CP phase δ^q , accompanied with two diagonal phase matrices P_u and P_d on both sides. However, as quarks are all Dirac fermions, the two phase matrices are unphysical at low energy.

Without loss of generality, we make a basis rotation to the basis where $U_u = U'_u = U'_l = 1$. This is done by performing 3×3 unitary transformations for $(\mathbf{10}, -\frac{1}{2})$, $(\bar{\mathbf{5}}, \frac{3}{2})$, $(\mathbf{1}, -\frac{5}{2})$ in their flavour space, respectively. Then, we arrive at

$$\begin{aligned} Y_u &= Y_\nu = \hat{Y}_u, \\ Y_d &= V_{\text{CKM}} \hat{Y}_d Y_{\text{CKM}}^T, \\ Y_l &= U_l \hat{Y}_l, \\ M_\nu &= U_l U_{\text{PMNS}} \hat{M}_\nu U_{\text{PMNS}}^T U_l^T, \\ M_{\nu^c} &= \hat{Y}_u U_l^* U_{\text{PMNS}}^* \hat{M}_\nu^{-1} U_{\text{PMNS}}^\dagger U_l^\dagger \hat{Y}_u \langle h_u \rangle^2. \end{aligned} \quad (35)$$

In this basis, Y_u and Y_d are fully fixed. The rest of the Yukawa mass matrices depend on U_l , the only undetermined unitary matrix involved in their flavour structures. Below, we discuss two extreme cases with U_l fixed.

- S1) $U_l = \mathbf{1}$. This case forbids the decays $p \rightarrow K^0 \mu^+$ and $p \rightarrow K^0 \mu^+$. The branching ratios for the remaining channels are predicted to be

$$\begin{aligned} \text{BR}(p \rightarrow \pi^0 e^+) &= 0.32, \\ \text{BR}(p \rightarrow K^0 e^+) &= 0.006, \\ \text{BR}(p \rightarrow \pi^+ \bar{\nu}) &= 0.68. \end{aligned} \quad (36)$$

The Yukawa mass matrices are simplified to

$$\begin{aligned} Y_l &= \hat{Y}_l, \\ M_\nu &= U_{\text{PMNS}} \hat{M}_\nu U_{\text{PMNS}}^T, \\ M_{\nu^c} &= \hat{Y}_u U_{\text{PMNS}}^* \hat{M}_\nu^{-1} U_{\text{PMNS}}^\dagger \hat{Y}_u \langle h_u \rangle^2. \end{aligned} \quad (37)$$

A typical numerical pattern of M_{ν^c} is given by

$$|M_{\nu^c}| \simeq \begin{pmatrix} 2.60 \times 10^3 & 7.09 \times 10^4 & 2.32 \times 10^7 \\ 7.09 \times 10^4 & 5.87 \times 10^8 & 1.21 \times 10^{10} \\ 2.32 \times 10^7 & 1.21 \times 10^{10} & 8.32 \times 10^{13} \end{pmatrix} \text{ GeV}, \quad (38)$$

where $m_1 = 0.1$ eV is assumed and phases in P_l and P_ν are set at zeros. The eigenvalues for M_{ν^c} are given by

$$(M_{\nu_1^c}, M_{\nu_2^c}, M_{\nu_3^c}) \simeq (2.61 \times 10^3, 5.86 \times 10^8, 8.32 \times 10^{13}) \text{ GeV}. \quad (39)$$

We see in this case that the RH neutrinos are very hierarchical. Due to the uncertainty of the complex phases, the RHN masses can still vary in a wide range, but they are in general very hierarchical. This is shown in the upper panel in Fig 5,

where both normal ordering (NO) and inverted ordering (IO) for light neutrino masses are considered. The heaviest right-handed neutrino mass varies between 10^{13} and 10^{16} GeV, depending on the mass of the lightest active neutrino mass. To satisfy the perturbativity condition, a lower bound on the $B-L$ scale should be considered, i.e., $M_{B-L} \gtrsim M_{\nu_3^c}$. Some lower $B-L$ scale cases, e.g., $M_{B-L} = 10^5, 10^9$ GeV listed in Fig. 2, are not consistent with the upper bound.

S2) $U_l = U_{\text{PMNS}}^\dagger$. Branching ratios of proton decay channels are numerically given by

$$\begin{aligned} \text{BR}(p \rightarrow \pi^0 e^+) &= 0.22, \\ \text{BR}(p \rightarrow \pi^0 \mu^+) &= 0.080, \\ \text{BR}(p \rightarrow K^0 e^+) &= 0.004, \\ \text{BR}(p \rightarrow K^0 \mu^+) &= 0.002, \\ \text{BR}(p \rightarrow \pi^+ \bar{\nu}) &= 0.69. \end{aligned} \quad (40)$$

This case leads to

$$\begin{aligned} Y_l &= U_{\text{PMNS}}^\dagger \hat{Y}_l, \\ M_\nu &= \hat{M}_\nu, \\ M_{\nu^c} &= \hat{Y}_u \hat{M}_\nu^{-1} \hat{Y}_u \langle h_u \rangle^2. \end{aligned} \quad (41)$$

Here, the right-handed neutrino mass matrix M_{ν^c} is diagonal, with three eigenvalues have clear correlation with light neutrino masses $M_{\nu_1^c}$, $M_{\nu_2^c}$, and $M_{\nu_3^c}$ given by m_u^2/m_1 , m_c^2/m_2 , and m_t^2/m_3 , respectively. Taking $m_1 = 0.1$ eV in normal ordering, we obtain

$$(M_{\nu_1^c}, M_{\nu_2^c}, M_{\nu_3^c}) \simeq (2.61 \times 10^3, 6.23 \times 10^8, 7.81 \times 10^{13}) \text{ GeV}. \quad (42)$$

A general correlation for the RHN mass spectrum with the lightest neutrino mass is given in the lower panel of Fig. 5.

6 Gravitational Waves

Recently, a series of PTA collaborations [2–5] have reported their latest data set on stochastic gravitational wave background (SGWB) emissions which provide strong evidence of SGWB signals with low frequencies in the range of nanohertz (nHz). Metastable cosmic strings can provide a potential interpretation to the observed SGWB signal [6].

In the context of flipped $SU(5)$, the cosmic strings scenario is realised with the following sequence of events: First, the spontaneous symmetry breaking of $SU(5)$ to $SU(3)_c \times SU(2)_L \times U(1)_y$, achieved at a scale $M_{\text{GUT}} \sim 2 \times 10^{16}$ GeV, will produce heavy monopoles of immense density. They carry Z_3 colour magnetic charge and Z_2 electroweak magnetic charge [51], as well as minimal magnetic charge $\frac{1}{2g_y}$ under $U(1)_y$ and g_y is connected with g_{B-L} via Eq. (26). In order to avoid cosmological issues their density must be diminished. A dominant role for their elimination is played by the inflationary scenario with the inflaton being either a neutral singlet (such as the one appearing in the decomposition of

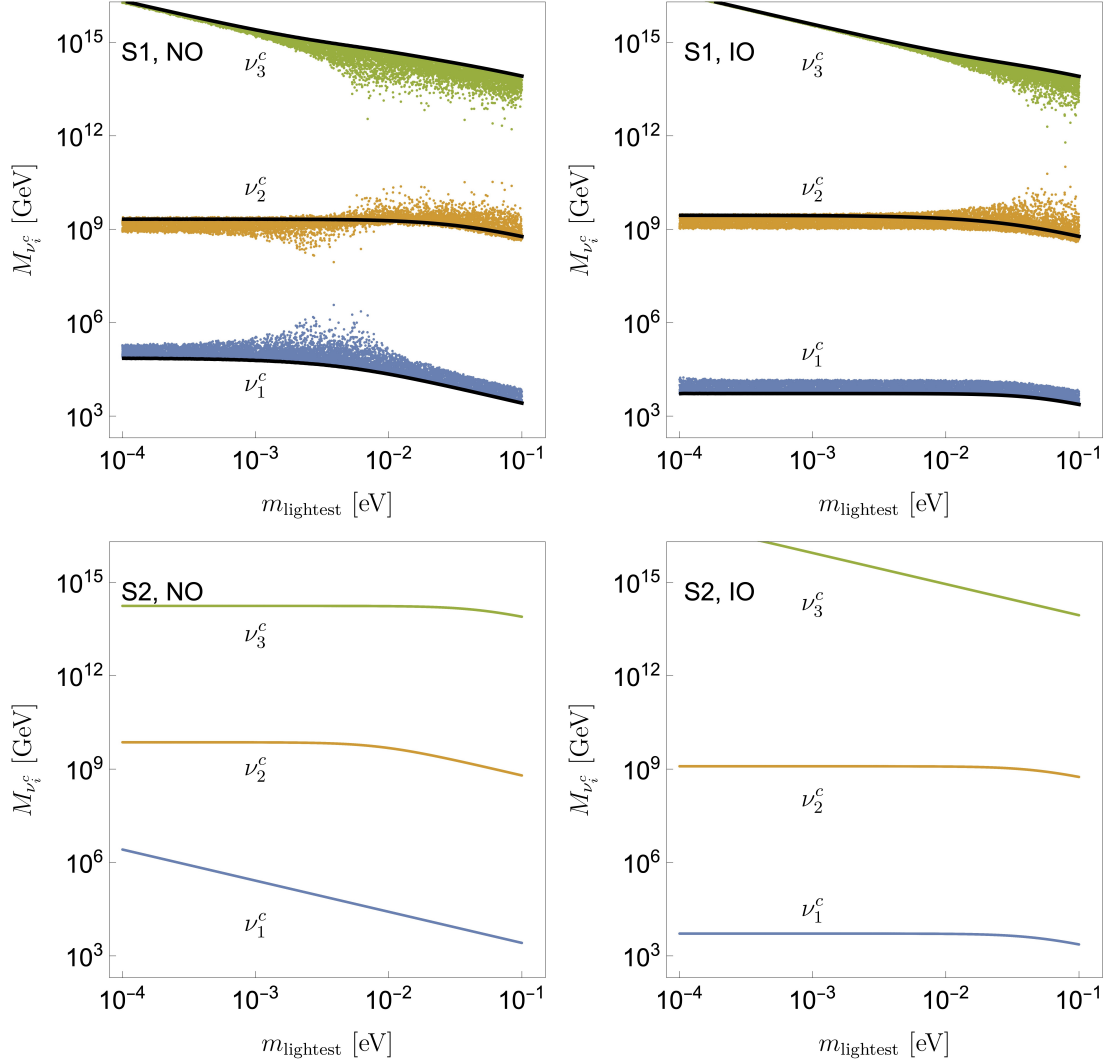


Figure 5: Prediction of RH neutrino mass spectrum vs the lightest active neutrino mass in normal ordering (NO, left panels) and inverted ordering (IO) of light neutrino masses. Black curves in the upper panels refer to all phases set to be zeros.

24 (see (3)) or by a modulus field which appears in the Kähler potential. In such a case, the scale of inflation can be around $\lesssim 10^{16}$ GeV just below M_{GUT} . During the period of inflation the monopoles are diluted and their density drops dramatically, making their current detection impossible.

Next, the spontaneous breaking of the $U(1)_\chi$ gauge factor at the high-scale M_{B-L} occurs where a network of long cosmic strings is copiously produced. According to the RGE analysis presented above, the scale M_{B-L} is somewhat lower than that of M_{GUT} .

Then, when such cosmic strings intersect, they form string loops which subsequently oscillate and through their decay emit Gravitational Waves. Superposition of GWs emitted by the various network's loops create a stochastic background in a wide frequency band. In the nHz range, it reproduces the experimentally observed low frequency signal [6].

The ratio of the GW energy density to the critical energy density ρ_c in the frequency

space is described by

$$\Omega_{\text{GW}}(f) = \frac{1}{\rho_c} \frac{d\rho_{\text{GW}}(f)}{d \log f} \quad (43)$$

It sums gravitational radiations from all strings loops in the past with redshift z on the frequency considered,

$$\Omega_{\text{GW}}(f)h^2 = \sum_{k=1}^{N_k} \frac{8\pi}{3} \left(\frac{h}{H_0} (G\mu)^2 \right)^2 P_k \frac{2k}{f} \int_0^\infty \frac{dz}{H(z)(1+z)^6} n(l(z, k), t(z)). \quad (44)$$

Here, $H_0 = 100h$ km/s/Mpc is the Hubble expansion rate today. In the early Universe, we use the Hubble expansion rate $H(z) = H_0 \sqrt{\Omega_\Lambda + \Omega_R(1+z)^3 + \Omega_M(1+z)^4}$ in the Λ CDM model with $\Omega_R = 9.1476 \times 10^{-5}$, $\Omega_M = 0.308$ and $\Omega_\Lambda = 1 - \Omega_R - \Omega_M$, where we have ignored the small correlation due to variation of the effective d.o.f. in the thermal bath for temperature above MeV scale. $P_k = \Gamma k^{-\frac{4}{3}} / \zeta(\frac{4}{3})$ (with $\Gamma \simeq 50$) describes the average gravitational radiation power from cusps in a loop respecting to the harmonic mode k in the loop oscillation [39]. We sum the k mode to a sufficiently large integer N_k in our calculation. In this work, we choose $N_k = 10^5$. $n(l, t)$ is the loop number density distribution function for loop length between $(l, l + dl)$ at time t , and the loop length l is correlated with the frequency today f via $l(z, k) = \frac{2k}{(1+z)f}$. In the case of stable strings, the simulation result obtained by assuming Nambu-Goto (NG) strings [40, 41] gives

$$n_{\text{NG}}(l, t) \simeq \frac{0.18}{(l/t + \Gamma G\mu)^{\frac{5}{2}} t^4} \theta(0.1 - l/t) \quad (45)$$

The GW spectrum predicted from stable strings depends mainly on one physical parameter $G\mu$. It is known that such a spectrum cannot explain the NANOGrav-15 signal [6]. This is simply explained below: The GW signal observed in NANOGrav requires a large $G\mu$ value to enhance the GW energy density; however, such large $G\mu$ provides only a relatively flat GW spectrum in the nHz band, which cannot match with the sharper power law indicated in the NANOGrav observation.

Metastable strings have been considered as an ideal explanation to the NANOGrav hint [42–44]. This scenario happens if the string formation energy scale $\sim \sqrt{\mu}$ is not far from the monopole mass scale. In such a case, the decay channel of strings to monopole-antimonopole pairs is open. This channel does not depend on the background of monopoles. It is worth mentioning that we do not change the timeline of the earlier history of the Universe. Namely, the $SU(5)$ is broken first, leading to the production of monopoles, which are then diluted by inflation. The process for cosmic strings forming from the $U(1)_{B-L}$ breaking is required in the end of the inflation. The low efficiency of monopole productions from string decays does not lead to cosmological problem. These monopoles do not carry unconfined fluxes after the electroweak breaking [45]. Note that although the $SU(5)$ scale is close the mass scale of $U(1)_{B-L}$ breaking, the time scale of topological monopole production from the $SU(5)$ breaking does not have to overlap with that of cosmic string generation from $U(1)_{B-L}$ breaking. A sufficiently long time gap between the two processes allows an insertion of a period of inflation to dilute away the monopole produced in the $SU(5)$ breaking and leave cosmic strings inside the horizon [46].

Due to the decay of the strings, the GW spectrum is suppressed in the lower frequency, leading to drop in the spectrum proportional to f^2 . We follow [47–50] to formulate the

GW spectrum from metastable strings. The instability of the string is described by a decay width per unit length Γ_d with an exponential suppression characterised by κ ,

$$\Gamma_d = \frac{\mu}{2\pi} e^{-\pi\kappa}, \quad \sqrt{\kappa} = \frac{M_{\text{GUT}}}{\alpha_5 \sqrt{\mu}}, \quad (46)$$

where the monopole mass has been approximated to M_{GUT}/α_5 by ignoring the order-one undermined factor [51]. For $\sqrt{\kappa} \gtrsim 9$, a string with sub-horizon length has a lifetime $t_s \simeq 1/\sqrt{\Gamma_d}$ comparable with the lifetime of the Universe and thus is considered as a stable string. For a smaller $\sqrt{\kappa}$ value, strings and loops can decay, and an exponentially suppression factor $e^{-\Gamma_d[l t + \frac{1}{2}\Gamma G\mu(t-t_s)^2]}$ should be included in the loop number density $n(l, t)$.

In Fig. 6, we show the predictions of key parameters of strings for our model. As the unification of $SU(3)_c$ and $SU(2)_L$ gauge couplings are insensitive to the $B - L$ scale. The string tension μ , which is proportional to M_{B-L}^2 , can vary in a large range up to the value referring to the GUT scale M_{GUT} . We set a bound for $\sqrt{\kappa} \lesssim 9$ for the instability of strings. Such a small value of κ requires energy scales of GUT breaking, inflation and $U(1)$ breaking not far away from each other, see [46] for inflationary model building in SUSY GUTs. In the right panel of Fig. 6, there is a small region, with $G\mu \sim 10^{-5}$, leading to metastable strings. This is higher than the typical values discussed recently, e.g., Refs. [42, 43] assumes $G\mu$ located somewhere around 10^{-6} or 10^{-7} .

In our case, in order to generate GWs consistent with NANOGrav 15 from oscillation of these heavier strings, inflationary period to dilute some of GWs at higher frequency is necessary, such that the LIGO/Virgo/KAGRA (LVK) bound $G\mu \lesssim 10^{-7}$ can be avoided. Including the influence of inflation is natural in the flipped $SU(5)$ as the energy scale of string generation scale is very close to the monopole scale. Thus, the string network is likely to form just in the last stage before the inflation is fully complete. Due to the influence of inflation, the string loops generated in the string network are firstly inflated and then re-enter the horizon at a certain time $t(z_{\text{inf}})$ respecting to the redshift z_{inf} . A simple treatment to including the influence of inflation is introducing a step function $\theta(t - t(z_{\text{inf}}))$.

Including all these effects together, we obtain the modified loop number density distribution function as

$$n(l, t) = n_{\text{NG}}(l, t) e^{-\Gamma_d[l t + \frac{1}{2}\Gamma G\mu(t-t_s)^2]} \theta(t - t(z_{\text{inf}})) \quad (47)$$

Taking it into Eq. (7), we are able to obtain GW spectrums compatible with NANOGrav signal and consistent with the LVK bound. We show three benchmarks of GW spectra in Fig. 7, with $z_{\text{inf}} = 10^{10}$, 10^{12} and 10^{14} assumed, referring to the time for strings re-enter the horizon at $t_{\text{inf}} = 0.26$, 3.6×10^{-5} and 3.8×10^{-9} second, respectively. Another curve of GW spectrum with strings not inflated by the inflation is shown for comparison, which conflicts with the LVK bound.

7 Conclusion

In this paper we have focused on the experimental tests of SUSY flipped $SU(5)$, including unification, proton decay, fermion masses and gravitational waves which arise from cosmic

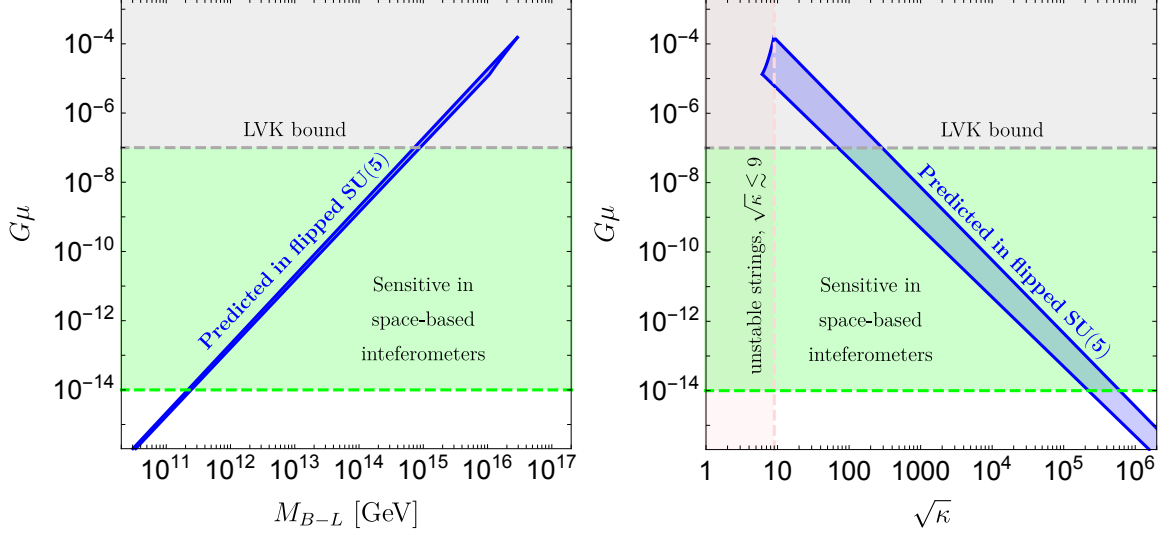


Figure 6: Prediction of the string tension, its correction with the scale M_{B-L} and the string stability in flipped $SU(5)$. In the right panel, $G\mu \lesssim 10^{-7}$ is set by current ground-based interferometers LVK for stable strings. Space-based interferometers such as LISA, Taiji and TianQin will have the ability to test GWs for strings with $10^{-14} \lesssim G\mu \lesssim 10^{-7}$, which is indicated in the green region of the plot. $\sqrt{\kappa}$ is the parameter representing the stability of strings, and strings with $\sqrt{\kappa} \lesssim 9$ are considered as unstable strings.

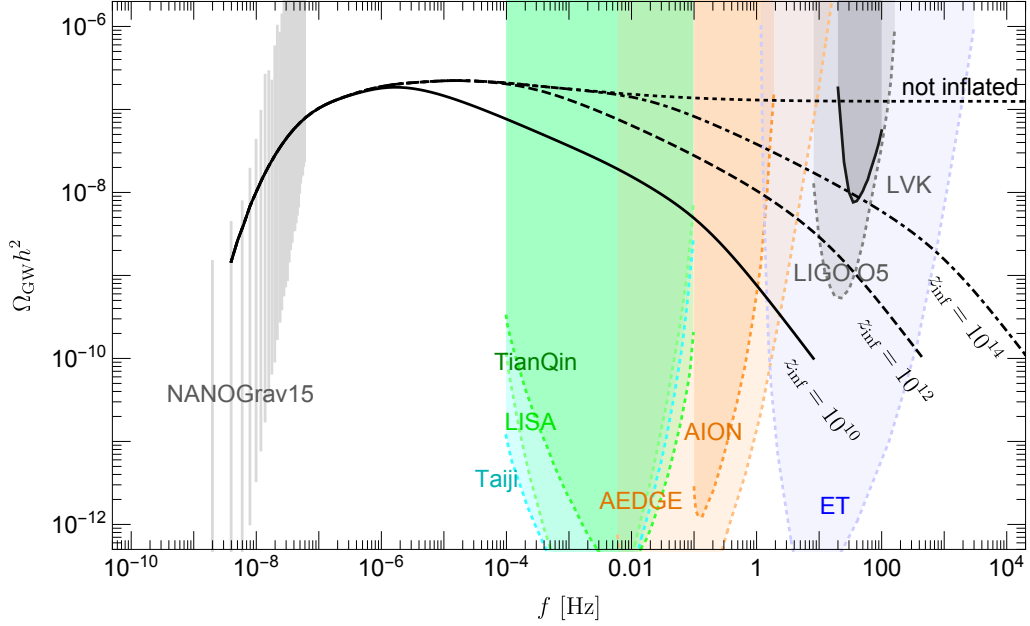


Figure 7: Benchmark of GW spectrums predicted in SUSY flipped $SU(5)$. $G\mu = 10^{-5}$ is used. $\sqrt{\kappa} = 7.8$ is tuned to fit the signal of NANOGrav 15 data in the nHz region. Three curves of GW spectrum with strings generated during the end of inflation are shown with strings re-entering the horizon at the redshift $z_{\text{inf}} = 10^{10}$, 10^{12} and 10^{14} , respectively. The k mode is summed up to $N_k = 10^5$. GW generated fully after inflation is shown in comparison.

string loops associated with the breaking of the high energy $U(1)_{B-L}$.

We have presented the spectrum of the model and described the breaking pattern of the flipped $SU(5) \times U(1)_\chi$ symmetry via a sequence of scales. We performed a two-loop

renormalisation group analysis for the gauge coupling unification of the $SU(5)$ factor. We found that the SUSY flipped $SU(5)$ model predicts a high GUT scale $M_{\text{GUT}} > 10^{16}$ GeV. We also investigated the restrictions on the M_{B-L} scale which is associated with the $U(1)_X$ breaking scale. We found that the M_{B-L} scale can vary in a broad region with negligible or little effect on the value of M_{GUT} .

Proton decay in this model is induced by dimension-6 operators only. The dimension-5 operator induced by SUSY contribution is suppressed due to the missing partner mechanism. We found that the partial decay width $p \rightarrow \pi^0 e^+$ is highly suppressed, being at least one order of magnitude lower than the future Hyper-K sensitivity. This suppression originates for two reasons: one due to the high GUT scale, the other because there are fewer dimension-6 operators compared with the traditional $SU(5)$ or $SO(10)$ models. Nevertheless we calculated all the decay channels of protons. The dominant channel is not $p \rightarrow \pi^0 e^+$ but $p \rightarrow \pi^+ \bar{\nu}$. The GUT scale is correlated with the SUSY breaking scale, but is insensitive to the $B - L$ breaking scale.

We also studied fermion (including neutrino) masses and mixings which can also influence proton decay. We presented two scenarios of flavour textures to check the consistency of the results with fermion masses and mixing.

The $B - L$ gauge breaking leads to the generation of cosmic strings. The $B - L$ scale here is not constrained by gauge coupling unification. If this scale is very close to that of GUT breaking, strings can be unstable due to the decay to monopole-antimonopole pair. Such metastable strings can be used to explain the NANOGrav signals of stochastic gravitational wave background, which may be interpreted here as resulting from the decay of metastable cosmic strings.

The present study complements previous recent studies where such testable predictions have been studied in the framework of $SO(10)$. Unlike the case of SUSY $SO(10)$ the SUSY breaking scale and the $U(1)_{B-L}$ breaking scales are essentially free parameters in flipped $SU(5)$, allowing for a wide range of gravitational wave signatures. This freedom allows the NANOGrav data to be fitted more easily in SUSY flipped $SU(5)$ than in SUSY $SO(10)$, for high $B - L$ breaking scales where unstable strings are possible, due to their decay into monopole-antimonopole pairs, without violating high frequency LIGO bounds. By contrast, in SUSY $SO(10)$, proton decay places a severe constraint on this scenario.

Acknowledgement

This work is supported by the STFC Consolidated Grant ST/L000296/1 and the European Union’s Horizon 2020 Research and Innovation programme under Marie Skłodowska-Curie grant agreement HIDDeN European ITN project (H2020-MSCA-ITN-2019//860881-HIDDeN) (S.F.K.), the Hellenic Foundation for Research and Innovation (H.F.R.I.) under the “First Call for H.F.R.I. Research Projects to support Faculty Members and Researchers and the procurement of high-cost research equipment grant” (Project Number: 2251) (G.K.L.), and National Natural Science Foundation of China (NSFC) under Grants No. 12205064 and Zhejiang Provincial Natural Science Foundation of China under Grant No. LDQ24A050002 (Y.L.Z.). G.K.L. would like to thank the staff of Nuclear and Parti-

cle Physics, of the Faculty of Physics of NKUA in Athens, for the kind hospitality where part of this work has been carried out. Y.L.Z would like to thank Y.L. Wu for useful discussions.

References

- [1] H. Georgi and S. L. Glashow, Phys. Rev. Lett. **32** (1974), 438-441 doi:10.1103/PhysRevLett.32.438
- [2] G. Agazie *et al.* [NANOGrav], Astrophys. J. Lett. **951** (2023) no.1, L8 doi:10.3847/2041-8213/acdac6 [arXiv:2306.16213 [astro-ph.HE]].
- [3] J. Antoniadis *et al.* [EPTA and InPTA:], Astron. Astrophys. **678** (2023), A50 doi:10.1051/0004-6361/202346844 [arXiv:2306.16214 [astro-ph.HE]].
- [4] D. J. Reardon, A. Zic, R. M. Shannon, G. B. Hobbs, M. Bailes, V. Di Marco, A. Kapur, A. F. Rogers, E. Thrane and J. Askew, *et al.* Astrophys. J. Lett. **951** (2023) no.1, L6 doi:10.3847/2041-8213/acdd02 [arXiv:2306.16215 [astro-ph.HE]].
- [5] H. Xu, S. Chen, Y. Guo, J. Jiang, B. Wang, J. Xu, Z. Xue, R. N. Caballero, J. Yuan and Y. Xu, *et al.* Res. Astron. Astrophys. **23** (2023) no.7, 075024 doi:10.1088/1674-4527/acdfa5 [arXiv:2306.16216 [astro-ph.HE]].
- [6] A. Afzal *et al.* [NANOGrav], Astrophys. J. Lett. **951** (2023) no.1, L11 doi:10.3847/2041-8213/acdc91 [arXiv:2306.16219 [astro-ph.HE]].
- [7] S. M. Barr, Phys. Lett. B **112** (1982), 219-222 doi:10.1016/0370-2693(82)90966-2
- [8] J. P. Derendinger, J. E. Kim and D. V. Nanopoulos, Phys. Lett. B **139** (1984), 170-176 doi:10.1016/0370-2693(84)91238-3
- [9] G. Charalampous, S. F. King, G. K. Leontaris and Y. L. Zhou, Phys. Rev. D **104** (2021) no.11, 115015 doi:10.1103/PhysRevD.104.115015 [arXiv:2109.11379 [hep-ph]].
- [10] J. Ellis, M. A. G. Garcia, N. Nagata, D. V. Nanopoulos and K. A. Olive, JHEP **05** (2020), 021 doi:10.1007/JHEP05(2020)021 [arXiv:2003.03285 [hep-ph]].
- [11] M. Mehmood, M. U. Rehman and Q. Shafi, JHEP **02** (2021), 181 doi:10.1007/JHEP02(2021)181 [arXiv:2010.01665 [hep-ph]].
- [12] I. Antoniadis, D. V. Nanopoulos and J. Rizos, JCAP **03** (2021), 017 doi:10.1088/1475-7516/2021/03/017 [arXiv:2011.09396 [hep-th]].
- [13] M. M. A. Abid, M. Mehmood, M. U. Rehman and Q. Shafi, JCAP **10** (2021), 015 doi:10.1088/1475-7516/2021/10/015 [arXiv:2107.05678 [hep-ph]].
- [14] J. Ellis, J. L. Evans, N. Nagata, D. V. Nanopoulos and K. A. Olive, Eur. Phys. J. C **81** (2021) no.12, 1109 doi:10.1140/epjc/s10052-021-09896-x [arXiv:2110.06833 [hep-ph]].

- [15] I. Antoniadis, D. V. Nanopoulos and J. Rizos, Eur. Phys. J. C **82** (2022) no.4, 377 doi:10.1140/epjc/s10052-022-10353-6 [arXiv:2112.01211 [hep-th]].
- [16] G. Lazarides, Q. Shafi and A. Tiwari, JHEP **05** (2023), 119 doi:10.1007/JHEP05(2023)119 [arXiv:2303.15159 [hep-ph]].
- [17] S. Basilakos, D. V. Nanopoulos, T. Papanikolaou, E. N. Saridakis and C. Tzerefos, Phys. Lett. B **849** (2024), 138446 doi:10.1016/j.physletb.2024.138446 [arXiv:2309.15820 [astro-ph.CO]].
- [18] B. Fu, S. F. King, L. Marsili, S. Pascoli, J. Turner and Y. L. Zhou, [arXiv:2308.05799 [hep-ph]].
- [19] B. Fu, S. F. King, L. Marsili, S. Pascoli, J. Turner and Y. L. Zhou, JHEP **11** (2022), 072 doi:10.1007/JHEP11(2022)072 [arXiv:2209.00021 [hep-ph]].
- [20] S. F. King, S. Pascoli, J. Turner and Y. L. Zhou, JHEP **10** (2021), 225 doi:10.1007/JHEP10(2021)225 [arXiv:2106.15634 [hep-ph]].
- [21] S. F. King, S. Pascoli, J. Turner and Y. L. Zhou, Phys. Rev. Lett. **126** (2021) no.2, 021802 doi:10.1103/PhysRevLett.126.021802 [arXiv:2005.13549 [hep-ph]].
- [22] S. Dimopoulos and H. Georgi, Nucl. Phys. B **193** (1981), 150-162 doi:10.1016/0550-3213(81)90522-8
- [23] I. Antoniadis, J. R. Ellis, J. S. Hagelin and D. V. Nanopoulos, Phys. Lett. B **194** (1987), 231-235 doi:10.1016/0370-2693(87)90533-8
- [24] B. Kyae and Q. Shafi, Phys. Lett. B **635** (2006), 247-252 doi:10.1016/j.physletb.2006.03.007 [arXiv:hep-ph/0510105 [hep-ph]].
- [25] H. Georgi and C. Jarlskog, Phys. Lett. B **86** (1979), 297-300 doi:10.1016/0370-2693(79)90842-6
- [26] S. Bertolini, L. Di Luzio and M. Malinsky, Phys. Rev. D **80** (2009), 015013 doi:10.1103/PhysRevD.80.015013 [arXiv:0903.4049 [hep-ph]].
- [27] M. Low and L. T. Wang, JHEP **08** (2014), 161 doi:10.1007/JHEP08(2014)161 [arXiv:1404.0682 [hep-ph]].
- [28] H. Fukuda, F. Luo and S. Shirai, JHEP **04** (2019), 107 doi:10.1007/JHEP04(2019)107 [arXiv:1812.02066 [hep-ph]].
- [29] S. Profumo, Phys. Rev. D **72** (2005), 103521 doi:10.1103/PhysRevD.72.103521 [arXiv:astro-ph/0508628 [astro-ph]].
- [30] G. F. Giudice and A. Romanino, Nucl. Phys. B **699** (2004), 65-89 [erratum: Nucl. Phys. B **706** (2005), 487-487] doi:10.1016/j.nuclphysb.2004.08.001 [arXiv:hep-ph/0406088 [hep-ph]].
- [31] J. Chakraborty, R. Maji, S. K. Patra, T. Srivastava and S. Mohanty, Phys. Rev. D **97** (2018) no.9, 095010 doi:10.1103/PhysRevD.97.095010 [arXiv:1711.11391 [hep-ph]].

- [32] S. P. Martin and M. T. Vaughn, Phys. Lett. B **318** (1993), 331-337 doi:10.1016/0370-2693(93)90136-6 [arXiv:hep-ph/9308222 [hep-ph]].
- [33] Z. z. Xing, H. Zhang and S. Zhou, Phys. Rev. D **86** (2012), 013013 doi:10.1103/PhysRevD.86.013013 [arXiv:1112.3112 [hep-ph]].
- [34] H. Murayama and A. Pierce, Phys. Rev. D **65** (2002), 055009 doi:10.1103/PhysRevD.65.055009 [arXiv:hep-ph/0108104 [hep-ph]].
- [35] H. S. Goh, R. N. Mohapatra, S. Nasri and S. P. Ng, Phys. Lett. B **587** (2004), 105-116 doi:10.1016/j.physletb.2004.02.063 [arXiv:hep-ph/0311330 [hep-ph]].
- [36] M. Severson, Phys. Rev. D **92** (2015) no.9, 095026 doi:10.1103/PhysRevD.92.095026 [arXiv:1506.08468 [hep-ph]].
- [37] A. Takenaka *et al.* [Super-Kamiokande], Phys. Rev. D **102** (2020) no.11, 112011 doi:10.1103/PhysRevD.102.112011 [arXiv:2010.16098 [hep-ex]].
- [38] Y. Aoki, T. Izubuchi, E. Shintani and A. Soni, Phys. Rev. D **96** (2017) no.1, 014506 doi:10.1103/PhysRevD.96.014506 [arXiv:1705.01338 [hep-lat]].
- [39] J. J. Blanco-Pillado and K. D. Olum, Phys. Rev. D **96** (2017) no.10, 104046 doi:10.1103/PhysRevD.96.104046 [arXiv:1709.02693 [astro-ph.CO]].
- [40] J. J. Blanco-Pillado, K. D. Olum and B. Shlaer, Phys. Rev. D **83** (2011), 083514 doi:10.1103/PhysRevD.83.083514 [arXiv:1101.5173 [astro-ph.CO]].
- [41] J. J. Blanco-Pillado, K. D. Olum and B. Shlaer, Phys. Rev. D **89** (2014) no.2, 023512 doi:10.1103/PhysRevD.89.023512 [arXiv:1309.6637 [astro-ph.CO]].
- [42] W. Buchmuller, V. Domcke and K. Schmitz, JCAP **11** (2023), 020 doi:10.1088/1475-7516/2023/11/020 [arXiv:2307.04691 [hep-ph]].
- [43] G. Lazarides, R. Maji, A. Moursy and Q. Shafi, [arXiv:2308.07094 [hep-ph]].
- [44] G. Lazarides and C. Pallis, Phys. Rev. D **108** (2023) no.9, 095055 doi:10.1103/PhysRevD.108.095055 [arXiv:2309.04848 [hep-ph]].
- [45] G. Lazarides, R. Maji and Q. Shafi, Phys. Rev. D **108** (2023) no.9, 095041 doi:10.1103/PhysRevD.108.095041 [arXiv:2306.17788 [hep-ph]].
- [46] S. Antusch, K. Hinze, S. Saad and J. Steiner, Phys. Rev. D **108** (2023) no.9, 095053 doi:10.1103/PhysRevD.108.095053 [arXiv:2307.04595 [hep-ph]].
- [47] W. Buchmuller, V. Domcke, H. Murayama and K. Schmitz, Phys. Lett. B **809** (2020), 135764 doi:10.1016/j.physletb.2020.135764 [arXiv:1912.03695 [hep-ph]].
- [48] W. Buchmuller, V. Domcke and K. Schmitz, Phys. Lett. B **811** (2020), 135914 doi:10.1016/j.physletb.2020.135914 [arXiv:2009.10649 [astro-ph.CO]].
- [49] W. Buchmuller, V. Domcke and K. Schmitz, JCAP **12** (2021) no.12, 006 doi:10.1088/1475-7516/2021/12/006 [arXiv:2107.04578 [hep-ph]].

- [50] M. A. Masoud, M. U. Rehman and Q. Shafi, JCAP **11** (2021), 022 doi:10.1088/1475-7516/2021/11/022 [arXiv:2107.09689 [hep-ph]].
- [51] J. Preskill, Ann. Rev. Nucl. Part. Sci. **34** (1984), 461-530 doi:10.1146/annurev.ns.34.120184.002333